DOI: 10.1002/chem.200600629

Antibiotic Resistance: Mono- and Dinuclear Zinc Complexes as Metallo-β-Lactamase Mimics

A. Tamilselvi, Munirathinam Nethaji, and G. Mugesh*[a]

Dedicated to Professor K. C. Nicolaou on the occasion of his 60th birthday

Abstract: Biomimetic systems containing one or two zinc(II) ions supported by phenolate ligands were developed as functional mimics of metallo-β-lactamase. These complexes were shown to catalytically hydrolyze β-lactam substrates, such as oxacillin and penicillin G. The dinuclear zinc complex **1**, which has a coordinated water molecule, exhibits high β-lactamase activity, whereas the dinuclear zinc complex **2**, which has no water molecules, but labile chloride ligands, shows a much lower activity. The high β-lactamase activity of complex **1** can be ascribed to the presence of a zinc-bound water molecule that is activated by being hydrogen bonded to acetate substituents. The kinetics of the hydrolysis of oxacillin by complex **1** and the effect of pH on the reaction rates are reported in detail. In addition, the kinetic parameters obtained for the synthetic analogues are compared with those of the natural metallo-β-lactamase from *Bacillus cereus* (BcII). To understand the role of the second metal ion in hydrolysis, the syntheses and catalytic activities of two mononuclear complexes (**3** and **4**) that include coordinated water molecules are described. Interestingly, the mononuclear zinc complexes **3** and **4** also exhibit high activity, supporting the assumption that the second zinc ion is not crucial for the β-lactamase activity.

Keywords: antibiotics · bioinorganic chemistry · enzyme models · penicillin · zinc

Introduction

Zinc, an essential and the second-most-abundant transition metal in biology, exerts its biological effect through several enzymes.[1] Apart from enzymes with one zinc-binding site, such as carbonic anhydrase and carboxypeptidase A, enzymes containing two or three zinc ions at the active sites are of current particular interest.[2] The most important and distinguishing features of these zinc enzymes are that the two metal ions are connected by bridging ligands with Zn···Zn distances ranging from 3.0 to 3.5 Å.[3] Metallohydrolases with dinuclear-zinc active sites perform many important biological hydrolytic reactions on a variety of substrates.[1,2] In this regard, metallo-β-lactamases (mβl, class B) represent a unique subset of zinc hydrolases that hydrolyze the β-lactam ring in several antibiotics (Scheme 1). The drug resistance that results from this hydrolysis is becoming an increased problem for the clinical community.[4] These metalloenzymes can hydrolyze a wide range of β-lactam substrates, such as cephamycins and imipenem, that are generally resistant to the serine-containing β-lactamases.[5,6] Therefore, the clinical application of the entire range of antibiotics is severely compromised in bacteria that produce metallo-β-lactamases.

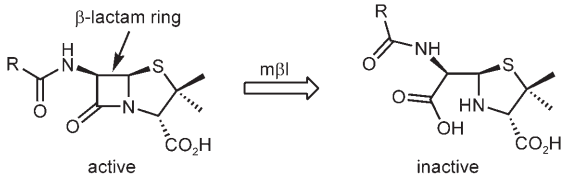

Scheme 1. Bacterial drug resistance: Hydrolysis of β-lactam antibiotics by metallo-β-lactamases (mβl).

Metallo-β-lactamases use one or two zinc ions in their active sites and are classified into three groups according to

[a] A. Tamilselvi, Dr. M. Nethaji, Dr. G. Mugesh
Department of Inorganic and Physical Chemistry
Indian Institute of Science, Bangalore 560 012 (India)
Fax: (+91) 80-2360-0683/2360-1552
E-mail: mugesh@ipc.iisc.ernet.in

Supporting information for this article is available on the WWW under http://www.chemeurj.org/ or from the author: Syntheses of ligands, results of ^{1}H NMR spectroscopic investigations of the hydrolysis of penicillin G, and HPLC data for the hydrolysis of oxacillin.

 © 2006 Wiley-VCH Verlag GmbH & Co. KGaA, Weinheim

Pagination corrected Oct. 17, 2006

their amino acid sequences.[4e,5a] The largest and most well-studied group of enzymes that belongs to the subclass B1 includes BcII from *Bacillus cereus*, CcrA from *Bacteroides fragilis* (Figure 1), and IMP-1 from *Pseudomonas aeruginosa*. The subclass B2 prototype enzyme is CphA from *Aeromonas hydrophila*, which differs considerably from other enzymes in its zinc dependence and substrate specificity. The third subclass B3 includes the L1 enzyme from *Stenotrophomonas maltophilia*, which is the only tetrameric mβl described so far. The crystal structures of several mβl entities reveal a unique αβ/βα sandwich fold in which the catalytic zinc-binding site lies at the interface between the two domains. However, the role of the additional zinc in the binuclear enzymes is still a matter of debate, as mononuclear enzymes generally display hydrolytic activity comparable with that of the binuclear enzymes.[7]

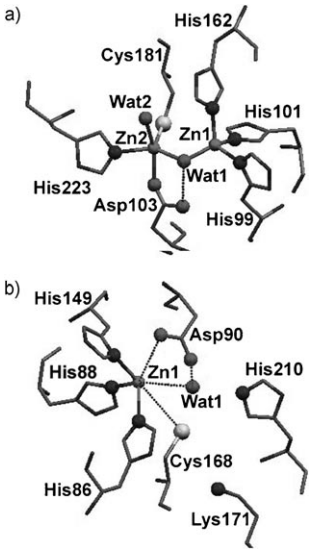

Figure 1. The active site of a) binuclear zinc enzyme from *B. fragilis* (PDB code: 1ZNB) and b) mononuclear zinc enzyme from *B. cereus* (PDB code: 1BMC).

Recently, a great deal of effort has been devoted to the development of zinc complexes as mimics of mβl entities.[8] In their pioneering work, Lippard and co-workers showed that zinc complexes having mono- and dinuclear active centers can catalyze the hydrolysis of penicillin G and nitrocefin.[8b] They also demonstrated that the bridging hydroxide in the dinuclear zinc(II) complex acts as the nucleophile in hydrolysis, and that the carboxylate group of these antibiotics is used for favorable positioning of the substrate and the nucleophile. Meyer and co-workers, on the other hand, investigated the hydrolytic cleavage of penicillin G mediated by pyrazolate-based dinuclear zinc complexes and showed that the cooperative effects of the adjacent metal ions might be operative, although they either enhance or diminish the β-lactamase activity with respect to free mononuclear zinc.[8d] Another exciting development in this area is the conversion of glyoxalase II into metallo-β-lactamase by extensive sequence changes, including the deletion and insertion of several structural loops in the active site. The resulting enzyme, evMBL8 (evolved metallo-β-lactamase 8), completely loses its original activity and, instead, catalyzes hydrolysis of a β-lactam substrate, cefotaxime.[9] In this paper, we describe a series of novel mono- and dinuclear zinc complexes as functional mimics of mβl entities. In addition, we describe the presence of a free tertiary amino substituent in close proximity to the zinc-bound water, which acts as a general base, promoting hydrolysis by activating the water molecule.

Results and Discussion

The ligands HL^1–HL^3 (Figure 2) used in the present study were synthesized from *p*-cresol and *p*-bromophenol by using appropriate amines. The amino phenol ligands HL^1–HL^3 were chosen because these dinucleating systems can hold two zinc(II) ions together, mimicking the zinc environment at the active sites of metallo-β-lactamases, in which the two zinc ions are coordinated predominantly by histidine ligands. Suitably designed phenolate ligands with ethylene diamine arms strongly favor the formation of dimetallic com-

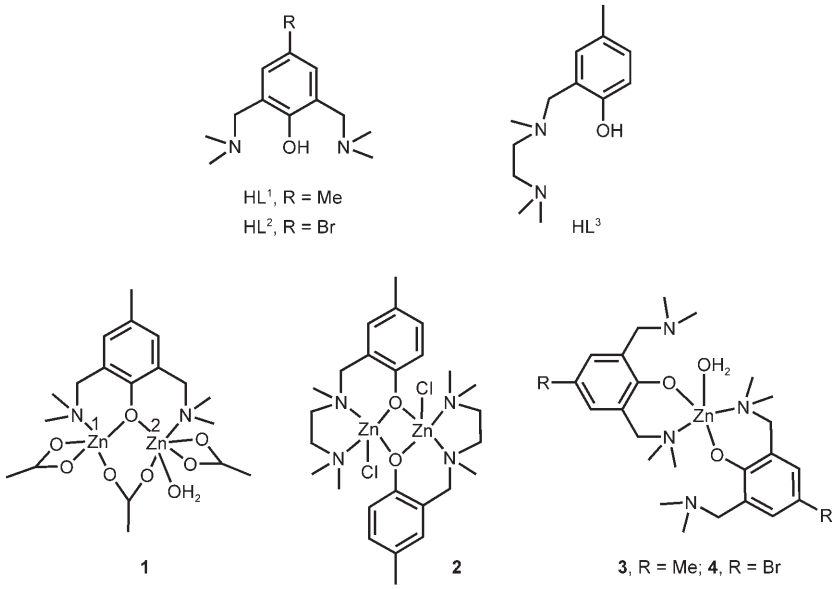

Figure 2. Chemical structures of ligands HL^1–HL^3 and complexes **1**–**4**.

 © 2006 Wiley-VCH Verlag GmbH & Co. KGaA, Weinheim

plexes.[10–13] Sorrel and co-workers reported some phenolate-bridged copper dimers as models for the active site of oxidized-hemocyanin derivatives and Karlin and co-workers utilized such ligands for modeling the copper monooxygenase systems.[10,13] Although there are several other examples of phenolate-bridged ligands,[14] only few of them have been used for hydrolytic reactions.[15] Uhlenbrock and Krebs reported the first example of a dizinc complex having a phenoxy bridge as a model for the dinuclear unit in the active site of phospholipase C.[16] Lippard and co-workers, on the other hand, reported an interesting class of dinuclear zinc(II) complexes having two ethylenediamine chelating ligands as functional mimics of metallo-β-lactamases.[8b]

Synthesis of the novel dinuclear zinc complex **1** (Figure 2) having a coordinated water molecule was achieved in good yield by treating the sodium salt of 2,6-bis[(dimethylamino)-methyl]-4-methyl phenol (HL^1) with $Zn(OAc)_2{\cdot}6H_2O$. The crystals suitable for single-crystal X-ray diffraction studies were obtained from a dichloromethane solution. The X-ray crystal structure of complex **1** reveals that the coordination geometry around the Zn1 ion differs from that of the other zinc ion (Zn2) (Figure 3). The first zinc ion (Zn1) is five-coordinate with four oxygen atoms and a nitrogen atom. The phenolate oxygen and an acetate ion act as bridging ligands, whereas the amino nitrogen and an asymmetric acetate group act as terminal ligands. The second zinc ion (Zn2), on the other hand, is six-coordinate with the same type of coordination, but in this case the sixth coordination site is completed by a water molecule. The Zn···Zn distance of 3.355(7) Å observed in complex **1** is significantly shorter than that of the binuclear zinc enzyme from *B. cereus* (3.848 and 4.365 Å),[3a] however, it is comparable with the corresponding distances in other binuclear enzymes, such as *S. maltophilia* (3.459 Å) and *B. fragilis* (3.457 Å).[3b,17] Complex **1** appears to be a good model for the active site of metallo-β-lactamases, because all three classes of metallo-β-lactamases mentioned above have a water molecule that coordinates to one of the zinc ions.

The synthesis of complex **1** was highly reproducible and the crystallization in dichloromethane by using different concentrations of the reaction product invariably afforded complex **1**. Because the stability constant of this complex is not expected to be very high, the acetates may dissociate and/or the dinuclear species may become mononuclear in solution. Therefore, the molecular structure of the complex in solvents, such as DMSO, in which the hydrolytic reactions were carried out (see below) may not be identical to that obtained from dichloromethane. To confirm the stability of complex **1** in solution, we carried out HPLC experiments in dichloromethane and in DMSO. These experiments show that the chromatograms obtained from the DMSO solution are identical to the ones obtained from the dichloromethane solution, indicating that complex **1** retains its dinuclear structure in solution. The peak areas obtained at different time intervals also suggest that the complex stays intact in solution (Figure S6b, Supporting Information).

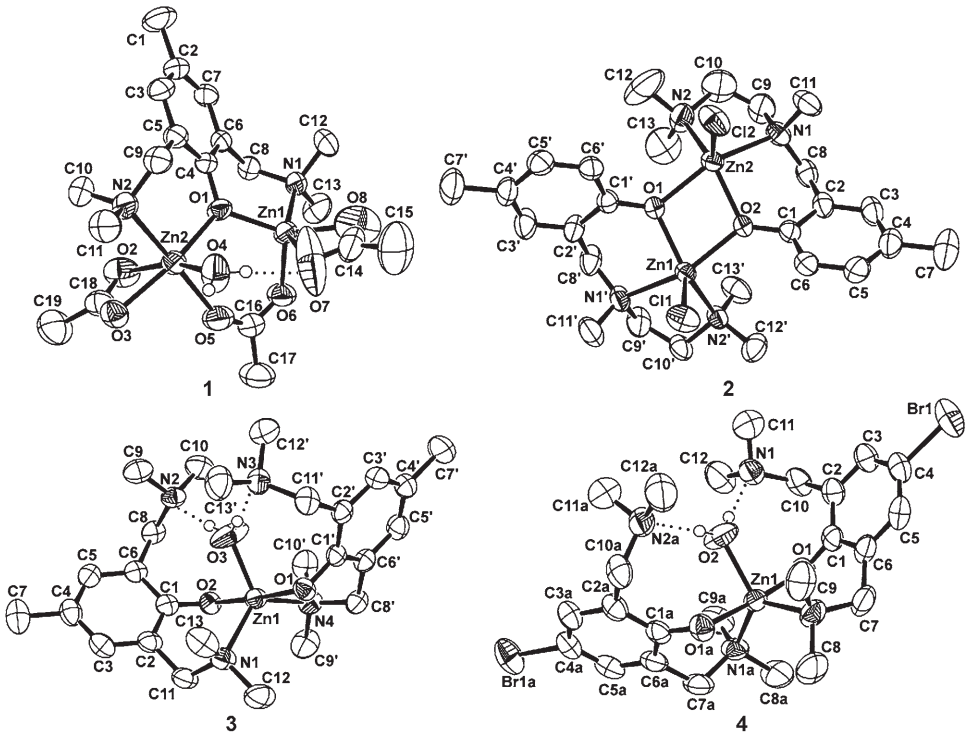

Figure 3. X-ray crystal structures of **1**–**4**. In **1**, the water molecule is hydrogen bonded to one of the acetate ligands, whereas in **3** and **4**, the water molecules are hydrogen bonded with the tertiary amino substituents. The hydrogen atoms (except those of water molecules) are omitted for clarity.

The other dinuclear zinc complex $[Zn_2(L^3)_2Cl_2]$ (**2**) (Figure 2) was synthesized by treating the amino phenol HL^3 with zinc chloride in the presence of triethylamine. The crystals suitable for X-ray analysis were obtained from a dichloromethane solution. In contrast to complex **1**, this compound crystallized as a symmetric dinuclear zinc complex with a Zn···Zn distance of 3.223 Å, which is significantly shorter than that of complex **1** (Figure 3). The two metal ions are held together by two phenolate bridging ligands and each metal ion is surrounded by two oxygen atoms, two nitrogen atoms, and a chloride ion. Notably, the presence of two ethylenediamine arms instead of just one in the *ortho* positions led to the isolation of dinuclear complexes having

 © 2006 Wiley-VCH Verlag GmbH & Co. KGaA, Weinheim

one phenolate and a hydroxyl, methoxy, or nitrate bridging ligand.[8b] The Zn···Zn distance observed in complex **2** is comparable with the corresponding distances in these zinc complexes, which range from 3.115 to 3.229 Å.[8b] In the syntheses of zinc complexes from zinc chloride, the nature of the ligands appears to have a large effect on the complex formation. If the reaction of zinc chloride was carried out with HL^1 instead of HL^3 (see Figure 3), we isolated a yellow compound that was a mononuclear species (**3**). Similarly, the reaction of HL^2 with anhydrous zinc chloride afforded another mononuclear complex (**4**) in moderate yield. The X-ray crystal structures of complexes **3** and **4** show trigonal-bipyramidal arrangements of the ligands around the metal center. Interestingly, in both complexes, one of the coordination sites around the zinc center is occupied by a water molecule (Figure 3). All attempts to prepare the corresponding dinuclear complexes by treating ligands HL^1 and HL^2 with zinc chloride were unsuccessful, although these ligands are known to be dinucleating species.

The dinuclear structures of complexes **1** and **2** and the observation of coordinated water molecules in complexes **1**, **3**, and **4** prompted us to study the hydrolytic behavior of these complexes. The β-lactamase activity of the metalloenzyme from *Bacillus cereus* and complexes **1**–**4** was studied by employing ^{1}H NMR spectroscopy and the reverse-phase HPLC method. Interestingly, complex **1** exhibited high β-lactamase activity by hydrolyzing the antibiotic substrate penicillin G (Scheme 1, R = Bz) at room temperature and a complete hydrolysis took place within 3 h, upon using 50 mM of the catalyst and 50 mM of the substrate (Figure S2, Supporting Information). Similarly, this complex was efficient in the hydrolysis of oxacillin, a penicillin analogue with high resistance to most of the serine-containing β-lactamases and, therefore, more stable than penicillin G toward hydrolysis. The hydrolyzed β-lactam products in these reactions were identical to the enzymatic reaction products, as evidenced from our ^{1}H NMR spectroscopic and HPLC analyses (Figure 4). The NH group of penicillin G and oxacillin was a useful probe for our ^{1}H NMR spectroscopic investigations. Treatment of complex **1** with penicillin G or oxacillin resulted in a complete change in the characteristic β-lactam signals, due to the hydrolytic cleavage of the four-membered ring. The nature of the hydrolyzed products was confirmed by comparing the NH and CH signals with those of the products obtained from the hydrolysis of penicillin G or oxacillin by the natural β-lactamase enzyme.

To find out whether complex **1** can act as a catalyst in the hydrolysis reaction, we undertook a detailed kinetic analysis. Interestingly, complex **1** was highly active at concentrations as low as 0.3 mol% (Figure S18 v–x, Supporting Information). The plots of percentage of oxacillin versus time for hydrolysis in the presence of **1** and some related compounds are given in Figure 5, and the corresponding t_{50} values (the time required for hydrolysis of 50% of the substrate) for oxacillin and penicillin G are summarized in Table 1. These data indicate that compound **1** rapidly hydrolyzes oxacillin and penicillin G with t_{50} values of 97 and 77 min, respectively, and these values are much lower than that of the control reaction ($t_{50} > 6300$ min for oxacillin and > 650 min for penicillin G). Furthermore, a complete hydrolysis of the substrates (100% hydrolysis) was observed with complex **1**. In contrast, a complete hydrolysis of the substrate was not observed with $Zn(OAc)_2{\cdot}2H_2O$ even after several days, although $Zn(OAc)_2{\cdot}2H_2O$ exhibited a significant initial reaction rate (Table 1, entry h) relative to the experiments not

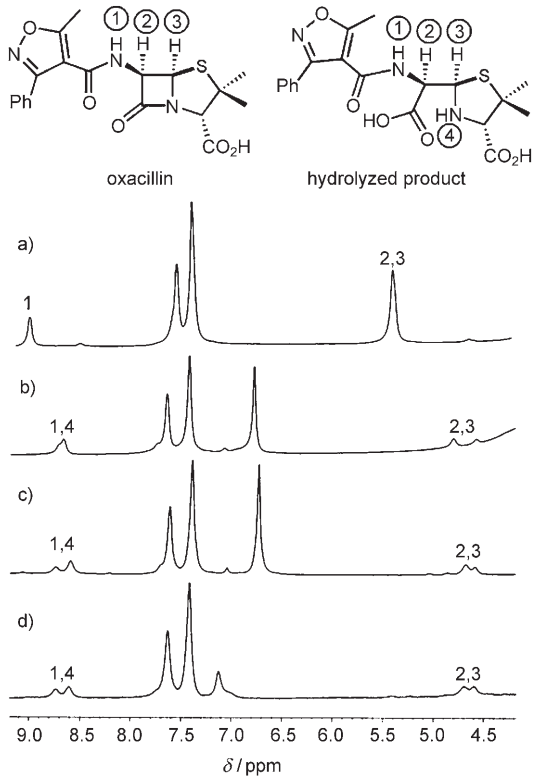

Figure 4. The NH and CH regions from the ^{1}H NMR spectra of a) oxacillin, b) an equimolar mixture of oxacillin and **1**, c) an equimolar mixture of oxacillin and **3**, and d) an equimolar mixture of oxacillin and **4**. The spectra were recorded in [D_6]DMSO at RT.

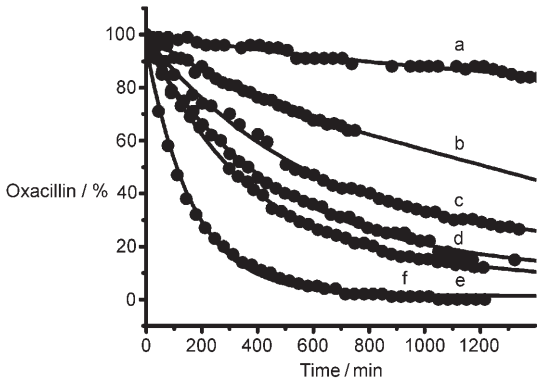

Figure 5. Hydrolysis of oxacillin (1.06×10^{-3} M) by a) HL^1, b) zinc acetate, c) **4**, d) **3**, e) **2**, f) **1** (each 2.1×10^{-5} M) in DMSO/HEPES buffer (1:9), pH 7.5. The reaction was monitored by reverse-phase HPLC and the amount of oxacillin hydrolyzed at any given time was calculated from the calibration plot.

 © 2006 Wiley-VCH Verlag GmbH & Co. KGaA, Weinheim

Table 1. The t_{50} values and initial rates (v_0) of hydrolyses of oxacillin and penicillin G by BcII, HL^1, $Zn(OAc)_2{\cdot}2H_2O$, and complexes **1**–**4** at RT.

Entry	Catalyst	Oxacillin		Penicillin G	
		t_{50} [min][a]	v_0 [μM min^{-1}][e]	t_{50} [min][a]	v_0 [μM min^{-1}][e]
a	control	>6300[b]	0.76	>650[f]	0.05
b	BcII	229	12.67	–	–
c	HL^1	>1940[c]	0.32	>650[g]	0.25
d	**1**	97	13.83	77	15.53
e	**2**	289	5.09	136	6.86
f	**3**	353	6.11	214	6.57
g	**4**	549	3.29	563	3.14
h	$Zn(OAc)_2{\cdot}2H_2O$	>750[d]	0.81	>700[h]	1.02

[a] Time required for 50% hydrolysis of substrate (t_{50}) was determined by monitoring the decrease in peak area due to oxacillin/penicillin G. [oxacillin]: 1.06×10^{-3} M; [penicillin G]: 1.00×10^{-3} M; [catalyst]: 2.12×10^{-5} M; in DMSO/HEPES buffer (1:9), pH 7.5; [BcII, class B enzyme from *B. cereus*]: 44.2 nM in HEPES buffer, pH 7.5. [b] After 6300 min, only 36% hydrolysis was observed. [c] After 1940 min, only 24% hydrolysis was observed. [d] After 750 min, only 36% hydrolysis was observed. [e] Calculated from the initial 5–10% of reaction by monitoring the decrease in peak area due to oxacillin. [f] After 650 min, only 4% hydrolysis was observed. [g] After 650 min, only 10% hydrolysis was observed. [h] After 700 min, only 26% hydrolysis was observed.

involving metal ions. Similarly, the free ligand (HL^1) did not show any noticeable activity, as the initial rate observed in the presence of HL^1 was almost identical to (penicillin G, Figure S17, Supporting Information) or even lower than (oxacillin) that of the control rate. With oxacillin as the substrate, only 24% hydrolysis was observed after 1940 min in the presence of HL^1 (Table 1, entry c) and 36% conversion was observed after 750 min in the presence of $Zn(OAc)_2{\cdot}2H_2O$ (Table 1, entry h). The natural enzyme (BcII, 44.2 nM), on the other hand, completely and effectively hydrolyzed oxacillin with a t_{50} value of 229 min. These observations also suggest that the simple metal salts are dissociated in solution to give free zinc ions that may be inhibited by the products, whereas the preorganized dinuclear zinc center in the natural enzyme and in complex **1** provides general base and single-site reactivity.

The remarkable catalytic activity of complex **1** can be ascribed to the tightly bound dinuclear zinc center and also to presence of an activated zinc-bound water molecule. It has been observed that the stability of the dizinc complexes in water is crucial for the hydrolytic activity of synthetic compounds. For example, certain active dinuclear zinc complexes that exhibit aminopeptidase activity are deactivated in the presence of water.[18] Therefore, the stability of the dinuclear metal center in complex **1** may account for its high reactivity. Furthermore, the analysis of the coordination environment around the zinc ions in complex **1** reveals that the water molecule coordinated to the Zn2 center is hydrogen bonded to the oxygen atom of the acetate ligand attached to Zn1 (O–H···O: 1.944 Å) (Figure 3), which may activate the water molecule toward hydrolysis. This observation is supported by the fact that one of the amino acid residues (Asp90) acts as the general base to abstract the proton from water and assist in hydrolysis.[19] Similar observations have been made for the hydroxylating activity of the diiron methane monooxygenase (MMO) enzyme in which the terminal water molecule attached to one of the iron ions is activated by Glu residues.[20] In agreement with this, the binuclear zinc complex **2** with no coordinated water or acetate ligands (Figure 3) shows much lower β-lactamase activity than that of **1**. The t_{50} values observed for complex **2** in the hydrolysis of oxacillin and penicillin G are three and two times, respectively, higher than that for complex **1**. A similar trend was observed in the initial rate of hydrolysis (Table 1).

To probe the role of the second metal ion in complex **1**, we carried out detailed hydrolysis experiments with the mononuclear zinc complexes **3** and **4** that have a water molecule as one of the ligands. The hydrolysis of penicillin G and oxacillin was monitored by ^{1}H NMR and/or HPLC methods. Interestingly, these complexes also hydrolyzed penicillin G (^{1}H NMR) and oxacillin (^{1}H NMR and HPLC) (Figures 4 and 5; Table 1), although the activity was less than that of the binuclear zinc complex **1**. The t_{50} values for the hydrolysis of oxacillin by **3** (353 min) and **4** (549 min) are higher than that of **1**, however, these values are very much lower than that of the control reaction (>6300 min). The initial rates (v_0) for the hydrolysis of oxacillin and penicillin G by **3** and **4** are higher than that of the control rate and also significantly higher than that of zinc acetate (Table 1). These observations support the previous results by Lippard and co-workers that the second metal ion is not crucial for β-lactamase activity.[8b] The greater activity of complexes **3** and **4** relative to that of free zinc ions is probably due to the presence of the coordinated water molecules that are involved in strong hydrogen bonding with the uncoordinated tertiary amino groups (Figure 3). The N···HO hydrogen-bonding distances in complexes **3** and **4** were 1.909 and 2.000 Å, respectively. These amino groups would certainly activate the water molecules to enhance the hydrolysis reaction.

The catalytic mechanism of Zn-containing enzymes requiring one metal ion for activity may become somewhat more efficient by acquisition of cocatalytic sites with two zinc ions in close proximity acting as a unit center.[21] However, the studies on the *B. fragilis* enzyme showed that the catalytic efficiency of the dinuclear enzyme is only marginally superior to that of its mononuclear counterpart with some substrates, and is even lower with other ones.[3d] Recent studies on functional analysis of the active-site residues reveal that two amino acids residues, Asp90 and His210, form a catalytic center with the zinc-bound water molecule, in which Asp90 acts as a general base in the enzymatic process. Further studies reveal that the proton-transfer process[22] from zinc-bound water to His210 readily occurs through a water-assisted pathway with an estimated barrier of around 8 kcal mol^{-1}.[19a,b] The proton abstraction by the histidine residue converts the water molecule into a more reactive hydroxo species, facilitating hydrolysis of the β-lactam ring. Based on these observations, it is clear that the uncoordinated amino substituent in complexes **3** and **4** acts as a general base in the reaction. This further supports the assumption

 © 2006 Wiley-VCH Verlag GmbH & Co. KGaA, Weinheim

that residues Asp90 and His210, which are involved in coordination with the second zinc in *B. cereus* (Figure 6), would play the role of the second zinc in mononuclear β-lactamases by activating the water molecules (Figure 1b).

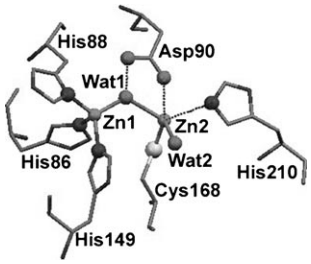

Figure 6. Active site of binuclear zinc enzyme from *B. cereus* (BcII, PDB code: 1BC2).

To understand the catalytic hydrolysis of β-lactam substrates by the synthetic compounds, and the effect of catalyst and substrate concentration on the reaction rates, we carried out further experiments by using oxacillin as the substrate. The rate of increase in the product formation was monitored by the reverse-phase HPLC method and the chromatograms were obtained at 254 nm, at which the hydrolyzed product showed a maximum absorbance. These measurements were recorded at various concentrations of complex ranging from 3.3 to 20 μM (Table 1) by keeping the substrate concentration constant. The initial rates were obtained graphically from the time course of each experiment. These results show that complex **1** is active in the hydrolysis of oxacillin at concentrations as low as 0.3 mol%. In other words, complex **1** catalyzes the complete hydrolysis of at least 300 equivalents of oxacillin substrate. Upon performing these experiments at different concentrations of complex **1**, a steady increase in the rate was observed as concentration increased. The initial rates (v_0) obtained at various concentrations of **1** are summarized in Table 1. The plot of initial rates against the catalytic concentration gave a straight line, indicating that β-lactamase activity is linearly proportional to the concentration of catalyst (Figure 7).

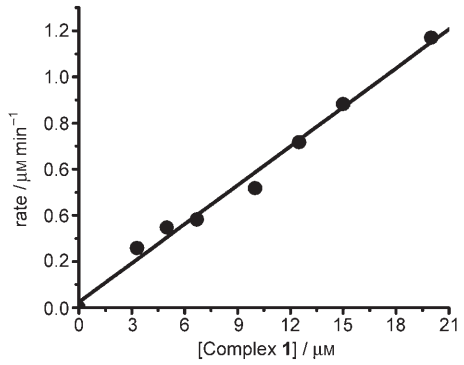

Figure 7. Effect of catalyst concentration on the hydrolysis of oxacillin by **1** (values taken from Table S20a). Initial rates were determined by monitoring the increase in peak area due to formation of hydrolyzed oxacillin turnover product, and were corrected for their background rates; [oxacillin] = 1.06×10^{-3} M in DMSO/HEPES buffer (1:9), pH 7.5.

Therefore, the initial rate is first order with respect to the complex concentration and hydrolysis may take place in a bimolecular fashion, analogous to the hydrolysis of penicillin catalyzed by $[Zn(cyclen)(OH)]^+$ in aqueous solution.[8a] However, our further studies indicate that the substrate binds more tightly to the complex, as evidenced from the low Michaelis constant (K_m) (see below), indicating an initial binding of the substrate, followed by intramolecular hydrolysis by the coordinated water/hydroxide.

As the catalyst (**1**) concentration was kept constant and the substrate (oxacillin) concentration was increased, a rapid increase in rate was observed in the initial stages, however, as the substrate concentration was increased further, the rate became constant, indicating that hydrolysis of oxacillin by the zinc complexes follows Michaelis–Menten kinetics. We next set out to determine kinetic parameters, such as the maximum velocity (V_{max}), Michaelis constant (K_m), turnover number (k_{cat}), and catalytic efficiency (η), for the hydrolysis reaction by carrying out several HPLC experiments at various concentrations of oxacillin. Double-reciprocal plots (Lineweaver–Burk plots) of initial rate versus substrate concentration yielded families of linear lines for all the complexes (Figure 8). The lines correspond to different catalysts and indicate that the rates increase linearly as concentration of the catalyst increases. The kinetic parameters obtained at several oxacillin concentrations are summarized in Table 2.

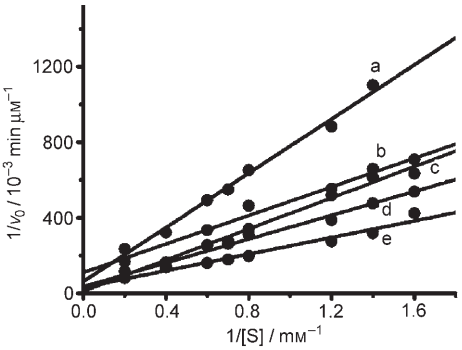

Figure 8. Lineweaver–Burk plots. Effect of substrate (oxacillin) concentration [S] on the lactamase activity of a) BcII, b) **1**, c) **3**, d) **2**, and e) **4**.

Interestingly, the Michaelis constants (K_m) for the dinuclear complexes **1** (8.94 μM) and **2** (3.43 μM) were much lower than those for the mononuclear complexes **3** (34.30 μM) and **4** (11.56 μM) under similar conditions, indicating that the binding of the substrate to the dinuclear complexes is much stronger than that to the mononuclear complexes. Furthermore, the K_m value for complex **1** in the presence of oxacillin is very similar to that of the dinuclear zinc enzymes BcII (6.97 μM) and IMP-1 (7.90 μM), but much lower than that of evMBL8 (Table 2), indicating that the binding of substrate to the dinuclear center of **1** is almost the same as that to the natural enzymes, but much stronger

 © 2006 Wiley-VCH Verlag GmbH & Co. KGaA, Weinheim

Table 2. The maximum rate (V_{max}), Michaelis constant (K_m), turnover number (k_{cat}), and catalytic efficiency (η) for the hydrolysis of oxacillin (**1**–**4**, BcII), and cefotaxime (evMBL8, IMP-1).

Complex	V_{max} [μM min^{-1}]	K_m [μM]	k_{cat} V_{max}/[catalyst] [min^{-1}]	η k_{cat}/K_m [M min^{-1}]
1	28.36	8.94	2.83	3.17×10^5
2	9.08	3.43	0.91	2.64×10^5
3	83.32	34.30	8.33	2.43×10^5
4	16.10	11.56	1.61	1.39×10^5
evMBL8[a]	–	229.00	2.52	0.11×10^5
IMP-1[a]	–	7.90	378.00	4.78×10^7
BcII[b]	31.64	6.97	717.20	10.29×10^7

[a] Äpparent kinetic parameters are taken from ref. [9]. [b] Initial concentration of BcII was fixed at 44.2 nM. All parameters listed are based on the initial rates determined at 25 °C.

than that to the engineered enzyme evMBL8. This is in accordance with the report of Rasia and Vila that states that the K_m values for the dinuclear native enzyme and their mutants from *B. cereus* are much lower than that of their mononuclear analogues.[23] Because the substrate binds to the dinuclear complexes more tightly than to the mononuclear ones (see below), saturation kinetics were easily observed for the dinuclear complexes. These observations suggest that the second zinc in the enzyme and also in the complexes plays some role in stabilizing the catalyst–substrate intermediate. These data also suggest that the dinuclear centers in complexes **1** and **2** stay intact in the hydrolysis, which is important for the binding of substrate, as suggested by Lippard and co-workers for the hydrolysis of nitrocefin.[8c]

In contrast, the k_{cat} value of the mononuclear zinc complex **3** is increased by 66% relative to that of the dinuclear complex **1**. This is due to the V_{max} value observed for complex **3** being higher than that of **1**. This indicates that the uncoordinated amino substituents in **3** may play important roles in hydrolysis. However, the overall catalytic efficiencies (η) derived from the k_{cat} and K_m values confirm that complex **1** is superior to other di- and mononuclear zinc complexes (**2**–**4**) in the present study. Crucially, the catalytic efficiency (η) of this particular complex for oxacillin (3.17×10^5 M^{-1}min^{-1}) is almost 30-times higher than that of evMBL8 for cefotaxime (0.11×10^5 M^{-1}min^{-1}),[9] and only 150- and 325-times lower than that of the dinuclear zinc enzymes IMP-1 and BcII, respectively (Table 2). These observations suggest that complex **1** has acquired a well-defined dinuclear metal coordination and a substrate-binding pocket for the metallo-β-lactamase activity. These data also suggest that the metal complexes exhibiting lower K_m and higher V_{max} are better catalysts for hydrolysis than the ones that exhibit higher K_m and lower V_{max} or higher K_m and V_{max} values. According to this, complex **1** is considered to be the most effective catalyst and complex **4** is considered to be the least effective catalyst in the present study, which is consistent with the t_{50} values for the hydrolysis of oxacillin and penicillin G by complexes **1** and **4** (Table 1).

To understand the effect of pH on the reaction rates, the initial rates were determined at various pH values. As expected, the catalytic activity was completely abolished at lower pH values and a rapid increase in the rate of hydrolysis was observed for complexes **1** and **3** at pH values above 7.0 (Figure 9). This is consistent with the observations of Lippard and co-workers that the rate-limiting nucleophilic

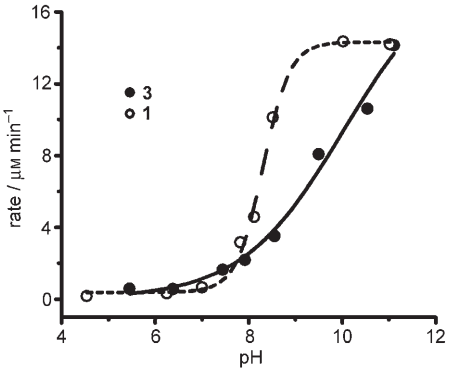

Figure 9. Effect of pH on the rate of hydrolysis of oxacillin by **1** and **3**.

attack of the hydroxo species on the substrate, followed by fast protonation of the intermediate, leads to the formation of the hydrolysis product.[24] Although the rate of reaction became constant at pH 8.5 for complex **1**, no such behavior was observed for complex **3**. In the case of **3**, a continuous increase in the rate was observed until pH 11.0, confirming the participation of the free tertiary amino substituents in hydrolysis. This is in agreement with the report of Bounaga and co-workers that protonation of the catalytically important Asp120 residue contributes to enzyme inactivation at acidic pH.[25] These data also suggest that the coordinated substrate may be attacked by an external hydroxide, leading to hydrolysis of the substrate. Rasia and Vila showed that the reversible inactivation of the enzyme at low pH may also be due to dissociation of the two zinc(II) equivalents.[23] The pH profile indicated that a second zinc(II) equivalent is not needed for nucleophile activation. Instead, the second zinc(II) may act to properly anchor Asp120, which ultimately orients the attacking nucleophile in dinuclear enzymes. They also suggested that the Arg121 residue may fulfil the role of the second zinc in the mononuclear enzymes.

Conclusion

We have shown that suitably substituted mono- and dinuclear zinc complexes can act as catalysts for the hydrolysis of β-lactam substrates, mimicking the properties of metallo-β-lactamases. This study suggests that the high reactivity of the complexes is due to the presence of zinc-bound water molecules that are activated by acetate or amino substituents. Our results support the assumption that the second zinc in the dinuclear enzymes does not participate directly in catalysis, but may orient the substrates for hydrolysis, and the basic amino acid residues, such as Asp and His, may ac-

 © 2006 Wiley-VCH Verlag GmbH & Co. KGaA, Weinheim

tivate the zinc-bound water molecules, fulfilling the role of the second zinc in the mononuclear enzymes. However, our HPLC results from the hydrolysis of oxacillin and penicillin G suggest that the second metal ion is required for a quantitative conversion of the substrates to the hydrolyzed products.

Experimental Section

General: Penicillin G (sodium salt) and oxacillin (sodium salt) were obtained from Fluka; captopril and penicillanase (β-lactamase II, BCII) from *Bacillus cereus* were obtained from Sigma. HEPES sodium salt, sodium hydride, deuterated solvents D_2O, CD_3OD, $[D_6]$DMSO, and $CDCl_3$ were obtained from Aldrich. *N*,*N*-dimethylamine, *N*,*N*,*N*′-trimethylethylenediamine, $Zn(OAc)_2{\cdot}2H_2O$, anhydrous zinc chloride, *p*-cresol, *p*-bromophenol, and 37% formaldehyde solution were obtained from other commercial sources and were used as received. HPLC-grade solvents for the kinetic experiments were obtained from Merck.

All chemical reactions were carried out under nitrogen or argon by using standard vacuum-line techniques. Solvents were purified by standard procedures and were freshly distilled prior to use. ^{1}H (400 MHz) and ^{13}C (100 MHz) NMR spectra were obtained by using a Bruker Avance 400 NMR spectrometer. Chemical shifts are cited in ppm with respect to $SiMe_4$ as internal (^{1}H and ^{13}C) standard. Infrared spectra were obtained as neat films by using a JASCO FTIR-410 spectrometer in the 4000–400 cm^{-1} regions. A Perkin–Elmer Lambda 5 UV/Vis spectrophotometer was used to measure the electronic absorption spectra. Mass spectral studies were carried out by using either a Q-TOF micro mass spectrometer with ESI-MS mode analysis or a FAB mass spectrometer. In the case of isotopic patterns, the value given is for the most intense peak. The syntheses of ligands HL^1, HL^2, and HL^3 were carried out by using standard protocols and are given in the Supporting Information.

Synthesis of $[Zn_2L^1(\mu\text{-}OAc)(OAc)_2(H_2O)]$ (1): The ligand HL^1 (0.222 g, 1 mmol) in dichloromethane (5 mL) together with 60% NaH (0.036 g, 0.9 mmol) in hexane (25 mL) were mixed and stirred at RT for 1 h to obtain the corresponding sodium phenolate (NaL^1). $Zn(OAc)_2{\cdot}2H_2O$ (0.329 g, 1.5 mmol) was then added and the stirring was continued for an additional 1 h. This resulted in a turbid solution from which the zinc complex $[Zn_2L^1(\mu\text{-}OAc)(OAc)_2(H_2O)]$ was filtered off as a white solid. The product was dried under vacuum to afford a white crystalline solid. The solid product was dissolved in dichloromethane and was kept for crystallization. Upon standing at RT, the product crystallized out as white needles suitable for X-ray analysis. Yield: 0.467 g (85%). ^{1}H NMR ($CDCl_3$): $\delta = 6.80$ (s, 2H), 3.73 (brs, 4H), 2.45 (brs, 12H), 2.38 (brs, 2H), 2.27 (s, 3H), 2.02 ppm (s, 9H); ^{1}H NMR ($[D_6]$DMSO): $\delta = 6.81$ (s, 2H), 3.51 (brs, 4H), 2.20 (brs, 12H), 2.15 (s, 3H), 1.83 ppm (s, 9H); ^{13}C NMR ($CDCl_3$): $\delta = 20.3$, 22.7, 46.2, 63.2, 122.4, 123.3, 124.7, 131.6, 132.5, 158.6, 180.3 ppm; IR (neat): $\tilde{\nu} = 3444$ (s), 3054 (w), 2975 (m), 2918 (m), 2849 (m), 2796 (m), 1744 (w), 1594 (vs), 1480 (m), 1456 (w), 1394 (m), 1338 (m), 1308 (m), 1282(w), 1151 (m), 1105 (w), 1047 (m), 1027 (s), 972 (m),932 (w), 875 (m), 799 (m), 767 (m), 734 (w), 678 (s), 619 (w), 566 (s), 405 cm^{-1} (m); MS (FAB): m/z: 469 $[Zn_2L^1(OAc)_2]^+$; elemental analysis calcd (%) for $C_{19}H_{32}N_2O_8Zn_2$ (547.25): C 41.70, H 5.89, N 5.12; found: C 41.94, H 6.11, N 5.22.

Synthesis of $[Zn_2(L^3)_2Cl_2]$ (2): Anhydrous $ZnCl_2$ (0.136 g, 1.0 mmol) in ethanol (10 mL) was added to a solution of the ligand HL^3 (0.222 g, 1.0 mmol) in ethanol (10 mL), and the reaction mixture was stirred for 30 min at RT. Triethylamine (257 μl, 2 mmol) was added to the reaction mixture and the stirring was continued for an additional 1 h. The resulting solution was concentrated to dryness under vacuum to afford a white solid. This was dissolved in dichloromethane and the mixture was allowed to evaporate slowly to obtain the compound **2** as white crystals. Yield: 0.346 g (54%). ^{1}H NMR ($CDCl_3$): $\delta = 2.24$ (s, 3H), 2.30 (s, 3H), 2.37 (s, 6H), 2.66 (s, 4H), 3.85 (s, 2H), 6.74 (d, $J = 8.4$ Hz, 1H), 6.78 (s, 1H), 6.95 ppm (d, 2H); IR (neat): $\tilde{\nu} = 3798$ (w), 3002 (m), 2981 (m), 2921 (m), 2732 (w), 2490 (w), 1612 (vs), 1494 (s), 1463 (m), 1417 (w), 1391 (w), 1345 (w), 1266 (vs), 1228 (m), 1168 (m), 1126 (m), 1104 (m), 1061 (m), 1010 (m), 975 (w), 939 (s), 835 (s), 792 (s), 732 (m), 757 (m), 699 (w), 672 cm^{-1} (w); MS (ESI): m/z: 643.2 $[Zn_2(L^3)_2Cl_2]^+$; elemental analysis calcd (%) for $C_{26}H_{42}N_4O_2Cl_2Zn_2$ (644.3): C 48.47, H 6.57, N 8.70; found: C 44.86, H 7.03, N 8.28.

Synthesis of $[Zn(L^1)_2(H_2O)]$ (3): The ligand HL^1 (0.287 g, 1 mmol) in dichloromethane (6 mL) together with 60% NaH (0.036 g, 0.9 mmol) in hexane (25 mL) were mixed and stirred at RT for 1 h to obtain the corresponding sodium phenolate (NaL^1). Anhydrous $ZnCl_2$ (0.137 g, 1.5 mmol) was added and the stirring was continued for an additional 1 h. The yellow turbid solution was filtered off to afford a clear solution, from which the yellow crystals suitable for X-ray analysis were obtained. Yield: 0.185 g (35%). ^{1}H NMR ($CDCl_3$): $\delta = 2.33$ (s, 6H), 2.29 (s, 24H), 3.50 (s, 8H), 6.83 ppm (s, 4H); IR (neat): $\tilde{\nu} = 3400$ (br), 2939 (m), 2853 (m), 2817 (m), 2774 (m), 1612 (w), 1473 (m), 1355 (w), 1321 (m), 1258 (w), 1033 (br, s), 871 (w), 841 (w), 792 (w), 606 (w), 459 cm^{-1} (s); MS (ESI): m/z: 508 $[Zn(L^1)_2]^+$; elemental analysis calcd (%) for $C_{26}H_{44}N_4O_3Zn$ (526.08): C 59.36, H 8.43, N 10.65; found: C 58.89, H 8.23, N 10.25.

Synthesis of $[Zn(L^2)_2(H_2O)]$ (4): The ligand HL^2 (0.287 g, 1 mmol) in dichloromethane (5 mL) together with 60% NaH (0.036 g, 0.9 mmol) in hexane (20 mL) were mixed and stirred at RT for 1 h to obtain the corresponding sodium phenolate (NaL^2). The resulting solution was treated with anhydrous $ZnCl_2$ (0.137 g, 1.5 mmol) and the stirring was continued for an additional 1 h. The resulting turbid solution was filtered off to afford a clear solution. The slow evaporation of the solvent afforded compound **4** as pale yellow crystals that were collected and dried. Yield: 0.269 g (41%). ^{1}H NMR ($CDCl_3$): $\delta = 2.29$ (br, 24H), 3.50 (s, 8H), 7.14 ppm (s, 4H); ^{13}C NMR ($CDCl_3$): $\delta = 165.3$, 155.1, 130.4, 124.8, 109.4, 101.8, 59.2, 44.2 ppm; IR (neat): $\tilde{\nu} = 2976$ (m), 2946 (m), 2853 (m), 2776 (m), 2341 (w), 1580 (m), 1456 (s), 1421 (s), 1363 (m), 1326 (m), 1289 (w), 1176 (m), 1150 (m), 998 (s), 982(m), 843 (m), 742 (m), 624 (m), 500 (w), 451 cm^{-1} (w); MS (FAB): m/z: 637 $[Zn(L^2)_2]^+$; elemental analysis calcd (%) for $C_{24}H_{38}Br_2N_4O_3Zn$ (655.78): C 43.96, H 5.84, N 8.54; found: C 44.22, H 5.99, N 8.39.

X-ray crystallography: X-ray crystallographic studies were carried out by using a Bruker CCD diffractometer with graphite-monochromatized $Mo_{K\alpha}$ radiation ($\lambda = 0.71073$ Å) controlled by a Pentium-based PC running the SMART software package.[26] Single crystals were mounted at RT on the ends of glass fibers and data were collected at 298 K. Intensity data were measured in frames with increasing ω (width of 0.3° per frame) at a scan speed of 18 s per frame and the SMART and SAINT software were used for data acquisition and data extraction, respectively. The structures were solved and refined by using the SHELXTL software package.[27] In general, all non-hydrogen atoms were refined anisotropically. Hydrogen atoms were assigned idealized locations. Empirical absorption corrections were applied to all structures by using SADABS.[28] The perspective views of the complexes were obtained by using PLATON[29] or ORTEP.[30] The coordination environments around the metal centers are given in Figure 3. CCDC-294711 (**1**), CCDC-294712 (**2**), CCDC-294713 (**3**), CCDC-294714 (**4**) contain the supplementary crystallographic data for this paper. These data can be obtained free of charge from The Cambridge Crystallographic Data Centre via www.ccdc.cam.ac.uk/data request/cif.

^{1}H NMR study on the hydrolysis of penicillin G and oxacillin by zinc complexes: The hydrolysis of penicillin G (Figures S1–4, Supporting Information) and oxacillin (Figure 4) was monitored by conducting ^{1}H NMR spectroscopy. All NMR experiments were carried out at 293 K. The chemical shifts are given in ppm relative to $[D_6]$DMSO as an internal reference. In each experiment, the test solution contained 0.05 μM of complex and 0.05 μM of either penicillin G sodium salt or oxacillin sodium salt. Pure $[D_6]$DMSO was used as the solvent in experiments investigating the binding of penicillin G with the complex.

Free penicillin G: ^{1}H NMR ($[D_6]$DMSO): $\delta = 8.84$ (d, 1H; C(O)N-amide), 7.33 (m, 5H; aromatic protons), 5.32 ppm (brs, 2H).

 © 2006 Wiley-VCH Verlag GmbH & Co. KGaA, Weinheim

Penicillin G in the presence of complex **1**: ^{1}H NMR ([D$_6$]DMSO): $\delta =$ 8.51 (1H; C(O)N-amide), 7.75 (m, 5H; aromatic protons) 4.47 (1H), 4.72 ppm (1H).

Penicillin G in the presence of complex **3**: ^{1}H NMR ([D$_6$]DMSO): $\delta =$ 8.31 (brd, 1H; C(O)N-amide), 7.22 (m, 5H; aromatic protons), 4.67 ppm (brd, 2H).

Penicillin G in the presence of complex **4**: ^{1}H NMR ([D$_6$]DMSO): $\delta =$ 8.45 (brd, 1H; C(O)N-amide), 7.18 (brs, 5H; aromatic protons), 4.51 ppm (brd, 2H).

Free oxacillin: ^{1}H NMR ([D$_6$]DMSO): $\delta = 9.07$ (d, 1H; C(O)N-amide), 7.52 (m, 5H; aromatic protons), 5.41 ppm (brs, 2H).

Oxacillin in the presence of complex **1**: ^{1}H NMR ([D$_6$]DMSO): $\delta = 8.65$ (1H; C(O)N-amide), 7.63 (brs, 2H; aromatic protons), 7.42 (brs, 3H; aromatic protons), 4.81 (1H), 4.59 ppm (1H).

Oxacillin in the presence of complex **3**: ^{1}H NMR ([D$_6$]DMSO): $\delta = 8.71$ (brd, 1H; C(O)N-amide), 7.64 (brs, 2H; aromatic protons), 7.42 (brs, 3H; aromatic protons), 4.65 ppm (brd, 2H).

Oxacillin in the presence of complex **4**: ^{1}H NMR ([D$_6$]DMSO): $\delta = 8.70$ (brd, 1H; C(O)N-amide), 7.63 (brs, 2H; aromatic protons), 7.42 (brs, 3H; aromatic protons), 4.68 ppm (brd, 2H).

Hydrolysis of penicillin G and oxacillin by β-lactamases: The hydrolyzed products from the reactions of penicillin G and oxacillin with test compounds were identical to those obtained by using the natural enzymes. For a comparison, both the binuclear metalloenzyme (BcII) and the serine-containing enzyme from *Bacillus cereus* were employed. The reactions were carried out in HEPES buffer at pH 7.5. In a typical experiment, 50 mg of oxacillin was dissolved in 10 mL of HEPES buffer and this solution was treated with one unit of BcII. After 30 min, the reaction afforded the expected hydrolyzed product, as confirmed by ^{1}H NMR spectroscopy and HPLC experiments. The reactions of oxacillin with the serine-containing β-lactamase, and of penicillin with both enzymes were performed by following the same procedure. The hydrolyzed products were purified by HPLC by using a semipreparative column and the solvent was evaporated under high vacuum. Oxacillin turnover product: ^{1}H NMR (400 MHz, CD_3OD): $\delta = 1.31$ (s, 3H), 1.60 (s, 3H), 2.69 (s, 3H), 3.60 (s, 1H), 4.54 (d, 1H), 5.20 (d, 1H), 7.48–7.49 (m, 3H), 7.86–7.87 ppm (m, 2H).

Determination of β-lactamase activity: The kinetics of hydrolysis of oxacillin and penicillin G were monitored by HPLC by using a reverse-phase column. All reactions with the natural enzymes were carried out in phosphate buffer and the reactions with synthetic compounds were carried out in a 9:1 mixture of 0.05 M HEPES buffer/DMSO at pH 7.5. The stock solutions of test complexes and oxacillin were prepared in the appropriate solvent and were used immediately to avoid any possible decomposition. The concentration of stock solutions of oxacillin, complexes, and inhibitor was fixed at 5×10^{-3} M. In a typical kinetics experiment, a sample vial containing 1.5 mL of the test complex and an appropriate concentration of oxacillin was incubated. At various time intervals, 10 μL aliquots were removed from the reaction mixture and injected directly onto the HPLC column. The compounds were eluted in a linear-gradient mode with a mixture of 30–80% acetonitrile and 0.1% trifluoroacetic acid (TFA) over 8.5 min at a flow rate of 1.0 mL min^{-1}. The reaction products (oxacillin turnover product, retention time: 3.66 min) and oxacillin (retention time: 4.24 min) were separable. The chromatograms were obtained at 254 nm and the concentration of oxacillin or hydrolyzed product was determined for each injection from the peak area by using a calibration plot. To avoid any significant changes in the concentrations of the starting materials or in the product inhibition, only the first 5–10% of conversion was monitored in most cases. To calculate the percentage conversion in the presence of the enzymes and complexes, the test samples were injected onto the column at regular time intervals and the HPLC was run for several hours. The maximum velocity (V_{max}), Michaelis constant (K_m), turnover number (k_{cat}), and catalytic efficiency (η) for each complex were calculated from the double-reciprocal or Lineweaver–Burk plots.

Acknowledgements

This study was supported by the Department of Science and Technology (DST) and the Council for Scientific and Industrial Research (CSIR), New Delhi, India. A.T. acknowledges the University Grants Commission (UGC), New Delhi, for a fellowship.

[1] a) D. E. Wilcox, *Chem. Rev.* **1996**, *96*, 2435–2458; b) W. N. Lipscomb, N. Sträter, *Chem. Rev.* **1996**, *96*, 2375–2433.

[2] a) N. Sträter, W. N. Lipscomb, T. Klabunde, B. Krebs, *Angew. Chem.* **1996**, *108*, 2158–2191; *Angew. Chem. Int. Ed. Engl.* **1996**, *35*, 2025–2055; b) H. Steinhagen, G. Helmchem, *Angew. Chem.* **1996**, *108*, 2489–2492; *Angew. Chem. Int. Ed. Engl.* **1996**, *35*, 2339–2342.

[3] a) J. A. Cricco, A. J. Vila, *Curr. Pharm. Des.* **1999**, *5*, 915–927; b) J. A. Cricco, E. G. Orellano, R. M. Rasia, E. A. Ceccarelli, A. J. Vila, *Coord. Chem. Rev.* **1999**, *190–192*, 519–535; c) Z. Wang, W. Fast, A. M. Valentine, S. J. Benkovic, *Curr. Opin. Chem. Biol.* **1999**, *3*, 614–622; d) Z. Wang, S. J. Benkovic, *J. Biol. Chem.* **1998**, *273*, 22402–22408.

[4] a) N. Sträter, W. N. Lipscomb, *Biochemistry* **1995**, *34*, 14792–14800; b) B. Chevrier, C. Schalk, H. D'Orchymont, J. M. Rondeau, D. Moras, C. Tarnus, *Structure* **1994**, *2*, 283–291; c) J. L. Vanhooke, M. M. Benning, F. M. Raushel, H. M. Holden, *Biochemistry* **1996**, *35*, 6020–6025; d) E. Hough, L. K. Hansen, B. Birknes, K. Jynge, S. Hansen, A. Hordvik, C. Little, E. Dodson, Z. Derewenda, *Nature* **1989**, *338*, 357–360; e) A. Volbeda, A. Lahm, F. Sakiyama, D. Suck, *EMBO J.* **1991**, *10*, 1607–1618.

[5] a) K. Bush, *Clin. Infect. Dis.* **1998**, *27*, S48–S53; b) D. M. Livermore, *J. Antimicrob. Chemother.* **1998**, *41*, 25–41.

[6] H. Kurosaki, Y. Yamaguchi, T. Higashi, K. Soga, S. Matsueda, H. Yumoto, S. Misumi, Y. Yamagata, Y. Arakawa, M. Goto, *Angew. Chem.* **2005**, *117*, 3929–3932; *Angew. Chem. Int. Ed.* **2005**, *44*, 3861–3864.

[7] R. Paul-Soto, M. Herández-Valladares, M. Galleni, R. Bauer, M. Zeppezauer, J.-M. Frére, H. W. Adolph, *FEBS Lett.* **1998**, *438*, 137–140.

[8] a) T. Koike, M. Takamura, E. Kimura, *J. Am. Chem. Soc.* **1994**, *116*, 8443–8449; b) N. V. Kaminskaia, B. Spingler, S. J. Lippard, *J. Am. Chem. Soc.* **2000**, *122*, 6411–6422; c) N. V. Kaminskaia, B. Spingler, S. J. Lippard, *J. Am. Chem. Soc.* **2001**, *123*, 6555–6563; d) B. Bauer-Siebenlist, S. Dechert, F. Meyer, *Chem. Eur. J.* **2005**, *11*, 5343–5352.

[9] H. Park, S. Nam, J. Lee, C. Yoon, B. Mannervik, S. J. Benkovic, H. Kim, *Science* **2006**, *311*, 535–538.

[10] T. N. Sorrell, C. J. O'Connor, O. P. Anderson, J. H. Reibenspies, *J. Am. Chem. Soc.* **1985**, *107*, 4199–4206.

[11] T. Mallah, M.-L. Boillot, O. Kahn, J. Gouteron, S. Jeannin, Y. Jeannin, *Inorg. Chem.* **1986**, *25*, 3058–3065.

[12] E. E. Eduok, C. J. O'Connor, *Inorg. Chim. Acta* **1984**, *88*, 229–233.

[13] M. S. Nasir, B. I. Cohen, K. D. Karlin, *J. Am. Chem. Soc.* **1992**, *114*, 2482–2494.

[14] a) B.-H. Ye, X.-Y. Li, I. D. Williams, X.-M. Chen, *Inorg. Chem.* **2002**, *41*, 6426–6431; b) A. Erxleben, *Inorg. Chem.* **2001**, *40*, 208–213; c) C. K. Williams, N. R. Brooks, M. A. Hillmyer, W. B. Tolman, *Chem. Commun.* **2002**, 2132–2133.

[15] a) J. Chen, X. Wang, Y. Zhu, J. Lin, X. Yang, Y. Li, Y. Lu, Z. Guo, *Inorg. Chem.* **2005**, *44*, 3422–3430; b) A. Horn, Jr., I. Vencato, A. J. Bortoluzzi, R. Hörner, R. A. N. Silva, B. Spoganicz, V. Drago, H. Terenzi, M. C. B. de Oliveira, R. Werner, W. Haase, A. Neves, *Inorg. Chim. Acta* **2005**, *358*, 339–351; c) H. Sakiyama, K. Ono, T. Suzuki, K. Tone, T. Ueno, Y. Nishida, *Inorg. Chim. Acta* **2005**, *358*, 372–374.

[16] S. Uhlenbrock, B. Krebs, *Angew. Chem.* **1992**, *104*, 1631–1632; *Angew. Chem. Int. Ed. Engl.* **1992**, *31*, 1647–1648.

[17] N. O. Concha, B. A. Rasmussen, K. Bush, O. Herzberg, *Structure* **1996**, *4*, 823–836.

[18] H. Sakiyama, R. Mochizuki, A. Sugawara, M. Sakamoto, Y. Nishida, M. J. Yamasaki, *Chem. Soc. Dalton Trans.* **1999**, 997–1000.

[19] a) D. Suárez, Jr., K. M. Merz, *J. Am. Chem. Soc.* **2001**, *123*, 3759–3770; b) N. Díaz, D. Suárez, Jr., K. M. Merz, *J. Am. Chem. Soc.*

 © 2006 Wiley-VCH Verlag GmbH & Co. KGaA, Weinheim

2001, *123*, 9867–9879; c) M. D. Peraro, A. J. Vila, P. Carloni, *Inorg. Chem.* **2003**, *42*, 4245–4247.
[20] a) B. Singh, J. R. Long, F. F. de Biani, D. Gatteschi, P. Stavropoulos, *J. Am. Chem. Soc.* **1997**, *119*, 7030–7047; b) A. C. Rosenzweig, P. Nordlund, P. M. Takahara, C. A. Frederick, S. J. Lippard, *Chem. Biol.* **1995**, *2*, 409–418.
[21] a) R. B. Davis, E. P. Abraham, J. Melling, *Biochem. J.* **1974**, *143*, 129–135; b) E. G. Orellano, J. E. Girardini, J. A. Cricco, E. A. Ceccarelli, A. J. Vila, *Biochemistry* **1998**, *37*, 10173–10180.
[22] S. Bounaga, A. P. Laws, M. Galleni, M. I. Page, *Biochem. J.* **1998**, *331*, 61–68.
[23] R. M. Rasia, A. J. Vila, *J. Biol. Chem.* **2004**, *279*, 26046–26051.
[24] N. V. Kaminskaia, C. He, S. J. Lippard, *Inorg. Chem.* **2000**, *39*, 3365–3373.
[25] S. Bounaga, A. P. Laws, M. Galleni, M. I. Page, *Biochem. J.* **1998**, *331*, 703–711.
[26] SMART (Version 5.05), Bruker AXS: Madison, WI, **1998**.
[27] a) G. M. Sheldrick, SHELXTL (V97–2), Siemens Industrial Automation, Madison, WI, **1997**; b) G. M. Sheldrick, SHELX-97, Program for Crystal Structure Solution and Refinement, University of Göttingen, Göttingen (Germany), **1997**.
[28] G. M. Sheldrick, SADABS (Version 2), Multi-Scan Absorption Correction Program, University of Göttingen, Göttingen (Germany), **2001**.
[29] A. L. Spek, *J. Appl. Crystallogr.* **2003**, *36*, 7–13.
[30] C. K. Johnson, ORTEP, Report ORNL-5138, Oak Ridge National Laboratory, Oak Ridge, TN, **1976**.

Received: May 4, 2006
Published online: August 11, 2006

 © 2006 Wiley-VCH Verlag GmbH & Co. KGaA, Weinheim